第 35 卷第 9 期
2019 年 9 月

无 机 化 学 学 报
CHINESE JOURNAL OF INORGANIC CHEMISTRY

Vol.35 No.9
1678-1686

氧化镉改性石墨毡作为高性能的钒电池负极

肖钦豪[1] 汪 雷[1] 李 丹[2] 景文珩*,[1]

([1]南京工业大学材料化工国家重点实验室,化工学院,南京 211816)

([2]江苏加怡热电有限公司,常州 213200)

摘要：为了提高原始石墨毡(GF)对 V^{3+}/V^{2+}氧化还原反应的电催化活性和降低析氢反应对电池性能的影响,本文采用水热法将氧化镉(CdO)纳米颗粒负载于石墨毡表面,制备出改性石墨毡(CdO/GF)作为高性能的钒电池负极。通过扫描电镜(SEM)、X 射线衍射分析(XRD)进行表面形貌和物相分析得出:CdO 纳米颗粒均匀负载于石墨毡纤维表面;线性扫描伏安法(LSV)、循环伏安测试(CV)、交流阻抗谱测试(EIS)表明：相对于 GF,CdO/GF 有效抑制了析氢反应的活性,CdO/GF 对于 V^{3+}/V^{2+}氧化还原反应的电化学活性和可逆性有显著的提高,电荷转移阻抗也有明显的减小;单电池测试中,对比 GF,CdO/GF 的放电容量衰减速率有显著的下降,在 90 $mA\cdot cm^{-2}$ 的电流密度下的电压效率和能量效率提高了约 5%。在多次充放电循环过程中,CdO/GF 的催化性能显示出良好的稳定性。

关键词：钒电池；石墨毡；氧化镉；负极；析氢反应

中图分类号：O646.54 **文献标识码**：A **文章编号**：1001-4861(2019)09-1678-09

DOI:10.11862/CJIC.2019.200

CdO-Modified Graphite Felt as a High-Performance Negative Electrode for a Vanadium Redox Flow Battery

XIAO Qin-Hao[1] WANG Lei[1] LI Dan[2] JING Wen-Heng*,[1]

([1]*State Key Laboratory of Materials-Oriented Chemical Engineering, College of Chemical Engineering, Nanjing Tech University, Nanjing* 211816, *China*)

([2]*Jiangsu Jiayi Thermal Power Co., Ltd., Changzhou, Jiangsu* 213200, *China*)

Abstract: To improve the electrocatalytic activity of pristine graphite felt (GF) towards the V^{3+}/V^{2+} redox couple and reduce the impact of the hydrogen evolution reaction (HER) on battery performance, in this study, cadmium oxide (CdO) nanoparticles were loaded onto the surface of graphite felt fibers by the hydrothermal method to prepare a high-performance negative electrode of a VRFB. The results of scanning electron microscopy (SEM), X-ray diffraction (XRD) showed that CdO nanoparticles were uniformly loaded on the surface of graphite felt fibers; Linear sweep voltammetry (LSV), cyclic voltammetry (CV) and electrochemical impedance spectroscopy (EIS) results indicated that the activity of HER was significantly inhibited by the presence of CdO. Furthermore, the electrochemical activity and reversibility of cadmium-doped graphite felt (CdO/GF) for the V^{3+}/V^{2+} redox reaction were significantly improved, and the charge transfer resistance was also significantly reduced as compared with GF. In a single-cell test, compared to GF, the discharge capacity attenuation rate of CdO/GF significantly decreased, the voltage efficiency and energy efficiency of CdO/GF were enhanced by approximately 5% at a current density of 90 $mA\cdot cm^{-2}$. Moreover, the catalytic performance of CdO/GF showed good stability during constant current 100 charge-discharge tests.

Keywords: vanadium redox flow battery; graphite felt; cadmium oxide; negative electrode; hydrogen evolution reaction

收稿日期:2019-02-25。收修改稿日期:2019-07-05。

国家自然科学基金(No.21676139,21838005),江苏省高等教育自然科学基金(No.15KJA530001),青蓝工程中青年学术带头人项目,江苏省六大人才高峰(No.JNHB-036);江苏省自然科学基金(No.BK20160297)资助。

*通信联系人。E-mail:jingwh@njtech.edu.cn

0 Introduction

With the rapid development of the global economy in recent years, the demand for energy is increasing. Fossil fuels are currently the main source of energy, but because they are not renewable, resources are gradually being depleted. Additionally, fossil fuels cause severe pollution of the environment, global warming, and climate change, and therefore, there has been an urgent need to develop clean renewable energy sources such as those from water, wind, and the sun[1-3]. However, according to the changes in the natural environment, the usage of unstable and intermittent renewable energy is facing more challenges, and to compensate, large-scale energy storage technology has emerged[4-5]. The all-vanadium redox flow battery (VRFB) is a secondary battery that uses a pump to circulate vanadium ions of different valence states as a reaction substance. With its long cycle life, high security, no pollution to the environment, deep discharge, capacity that can be designed according to requirements, little cross-contamination, and other advantages, the VRFB has become one of the most promising electrochemical energy storage systems for renewable energy[6-7].

In spite of many outstanding advantages, there are still some drawbacks that restrict the commercial application of VRFBs. For example, VRFBs have lower energy density[8], the membrane of the VRFB has poor ionic selectivity, causing serious cross-contamination of the active species[9], and graphite felt has poor electrochemical activity and kinetics reversibility [10]. The electrode is where the battery reaction occurs, and the energy efficiency of a VRFB largely depends on the physicochemical properties of its electrodes[11]. Graphite felt (GF) is considered as a preferred electrode material for VRFB because of its large surface, high conductivity, high stability in strong acidic conditions, and low cost[3,12]. However, graphite felt has poor wettability and electrocatalytic activity, which originates from its hydrophobic property[13-14].

In order to address these problems, many studies have been devoted to the modification of graphite felt. The modification methods include: acid treatment [15], heat treatment[16], electrochemical oxidation treatment[17], surface metallization[18], non-metallic element treatment[19], *etc*. The acid treatment, heat treatment, and electrochemical oxidation treatment mainly increase the oxygen-containing functional groups on the surface of the graphite felt fibers to improve the hydrophilicity of the graphite felt and the adsorption capacity of the reactive material. The surface metallization treatment and non-metallic element treatment use an electrocatalyst (including metal and metal oxides and non-metallic materials) loaded with nanostructures on the surface of graphite felt fibers to increase the active sites for redox reactions[14].

At present, many studies have focused on the modification of the positive electrode of the VRFB[20-24], while the modification of the negative electrode of the VRFB involves very little effort[25]. As the poor performance of V^{3+}/V^{2+} redox reaction occurs in the negative side of the VRFB limiting the battery performance. Moreover, according to the reduction standard potential values of the reaction shown in reaction equations (**1**) and (**2**), The hydrogen evolution reaction (HER) is thermodynamically favorable.

$$V^{3+}+e^{-}\rightarrow V^{2+} \qquad E^{\ominus}=-0.26\ \text{V} \qquad (\mathbf{1})$$

$$2H^{+}+2e^{-}\rightarrow H_2 \qquad E^{\ominus}=0\ \text{V} \qquad (\mathbf{2})$$

This indicates that an irreversible reaction (HER) simultaneously occurred because of the reduction of V^{3+} at the negative electrode during the charge. As a result, V^{3+} was not entirely reduced to V^{2+}, whereas VO^{2+} was completely oxidized to VO_2^{+}, which forced the end of the charge. During the discharge, there was insufficient V^{2+} to balance VO_2^{+}. The HER is a parasitic process that consumes 5% to 50% of the current applied to a cell. The bubbles generated from it will reduce the liquid-phase volume in the electrodes, reducing the active surface area of the electrodes, and affecting the flow of the electrolyte. The HER will lead to unbalanced charging of the VRFB, an increase in battery polarization, and a decrease in battery performance[26-30]. Recently, some efforts have been made to inhibite the activity of the HER and improve the electrochemical activity of V^{3+}/V^{2+} redox reaction.

Especially, bismuth (Bi) was confirmed as excellent catalyst for V^{3+}/V^{2+} redox reaction. For instance, Li et al.[31] employed electrolytes containing Bi^{3+}, Bi nanoparticles are synchronously electrodeposited onto the surface of a graphite felt during operation of VRFB. In single cell test, the EE is increased by 11% at 150 $mA \cdot cm^{-2}$; Liu et al.[32] used bismuth to modified the GF by hydrothermal method. Experimental results shows that bismuth can effectively inhibit the side reaction of hydrogen evolution in wide temperature range, while promoting the V^{3+}/V^{2+} redox reaction.

Because cadmium (Cd) has a high hydrogen evolution overpotential, it can effectively inhibit the activity of the HER[33]. Additionally, cadmium oxide (CdO), as a semiconductor material, its special energy band structure can make it more difficult for the products formed by the reaction to adsorb onto the electrodes surface. Moreover, the oxidation rate of the electrode surface is higher than that of the general electrode[34]. Therefore, in this work, CdO was used as a catalyst to inhibit the activity of the HER and improve the electrocatalytic activity of graphite felt. Using a hydrothermal method, cadmium-doped graphite felt was successfully synthesized for the first time to act as a high-performance negative electrode of VRFB. The surface morphology and crystal structure of the graphite felt fibers were determined by scanning electron microscopy (SEM) and X-ray diffraction (XRD). The electrochemical activity of the electrodes was evaluated by linear sweep voltammetry (LSV), cyclic voltammetry (CV), and electrochemical impedance spectroscopy (EIS). Finally, VRFB performance was evaluated by the single-cell test. Moreover, a catalytic reaction mechanism for CdO in the redox reactions occurring in this negative half-cell is proposed.

1 Experimental

1.1 Electrode preparation

All chemicals were used directly without further purification. Polyacrylonitrile (PAN)-based graphite felt (6 mm thickness, Shanghai Hongsheng Industrial Co., Ltd.) was obtained, and pieces with dimensions of 3 cm×3.5 cm and 1 cm×1 cm were used as the electrodes. To avoid impurities and enhance wettability, untreated graphite felt was heat-treated in air at 400 ℃ for 2 h and then cooled to room temperature to obtain heat-treated graphite felt (GF). Cadmium-doped graphite felt (CdO/GF) was synthesized through a hydrothermal method as follows: 0.4 g $Cd(NO_3)_2 \cdot 4H_2O$ (Shanghai Jinshanting New Chemical Reagent Factory) was dissolved in 40 mL deionized water under stirring at room temperature. After stirring for 30 min, the solution was transferred to a 100 mL Teflon-lined autoclave, and the GF was immersed in the solution. After careful sealing, the autoclave was heated to 180 ℃ and maintained at temperature for 10 h. After the reaction, the autoclave was cooled to room temperature. The GF was removed from the autoclave, washed three times with deionized water, and dried in a drying oven at 70 ℃ for 12 h. In order to enhance the adhesion between GF and CdO, after the hydrothermal reaction, the sample was heat-treated at 400 ℃ for 1 h in an N_2 atmosphere.

1.2 Physicochemical characterization

The surface morphology of graphite felt fibers was observed by scanning electron microscope (Hitachi S-4800). The crystallographic structure of the samples was analyzed by X-ray diffraction (Miniflex 600X Japanese Science with Cu $K\alpha$ radiation (λ=0.154 nm) at 40 kV and 15 mA), and scanning between 5° and 80° (2θ) at a scan rate of $10° \cdot min^{-1}$.

1.3 Electrochemical characterization

The electrochemical performance of prepared electrodes was examined using an electrochemical workstation (Gamry Reference 3000). The linear sweep voltammetry (LSV), cyclic voltammetry (CV), and electrochemical impedance spectroscopy (EIS) were performed using a three-electrode setup consisting of CdO/GF (1 cm×1 cm) as the working electrode, a platinum sheet as the counter electrode, and a saturated calomel electrode (SCE) as the reference electrode. The LSV test was carried out in the potential range between −1.5~0 V at a scan rate of 5 $mV \cdot s^{-1}$ in 0.05 $mol \cdot L^{-1}$ Na_2SO_4 solution. The CV test was conducted between −1 V and 0 V at a scan rate of 5 $mV \cdot s^{-1}$ in 0.1 $mol \cdot L^{-1}$ $VOSO_4$ and 3 $mol \cdot L^{-1}$ H_2SO_4

electrolyte solution. In addition, the EIS test was carried out under open circuit potential (OCP) in 0.1 mol·L^{-1} $VOSO_4$+3 mol·L^{-1} H_2SO_4 with a sinusoidal AC signal of 10 mV in the frequency range of 10^5~10^{-2} Hz. All tests were performed and conducted at room temperature, and nitrogen was introduced during the test to create inert conditions. GF was also tested under the same conditions for comparison.

1.4 VRFB single-cell evaluation

The VRFB performance was evaluated with a BTS-5V6A battery tester (Shenzhen Newware Technology Electronics Co., Ltd.) using a constant current charge-discharge test. The single cell was equipped with a Nafion 117 perfluorinated ion-exchange membrane (Dupont, USA) as the separator, two pieces of graphite felt with a size of 3 cm×3.5 cm as the electrodes, and graphite plates as the current collector. The initial electrolyte was prepared by dissolving $VOSO_4·3H_2O$ (Nanjing Kangmanlin Chemical Industry Co., Ltd.) in H_2SO_4 solution. Other V solutions with different valance states were obtained by electrolyzing the initial solution. Negative and positive electrolytes (15 mL in each half-cell) consisted of 1.5 mol·L^{-1} V^{3+}/V^{2+} and 1.5 mol·L^{-1} V^{5+}/V^{4+} in 3.0 mol·L^{-1} H_2SO_4, respectively. The electrolyte was stored in a glass container outside the cell and circulated by a peristaltic pump (BT100-1L Baoding Lange Constant Flow Pump Co., Ltd.) with an electrolyte flow rate of 25 mL·min^{-1}. The upper limit of the charge voltage and lower limit of the discharge voltage were 1.75 V and 0.75 V, respectively. In addition, N_2 was introduced into the negative side to maintain an inert atmosphere during the investigation.

2 Results and discussion

2.1 Physicochemical characterization

The surface morphology of GF and CdO/GF was studied by SEM. Fig.1(a,b) shows the morphology of GF, consisting of a smooth surface with no impurities on it, and clearly visible gullies. Fig.1(c,d) shows the morphology of CdO/GF, and it can be seen that a large amount of particles with a homogeneous diameter of 300~400 nm was uniformly loaded on the surface of the CdO/GF, with no severe agglomeration.

The crystal structures of the samples were investigated by XRD. Fig.2 shows the XRD patterns of GF and CdO/GF. It can be seen from the comparison that GF and CdO/GF both have unique and broad characteristic peaks at 25.1°and 43.2°, corresponding to the crystallographic planes (002) and (004) of the

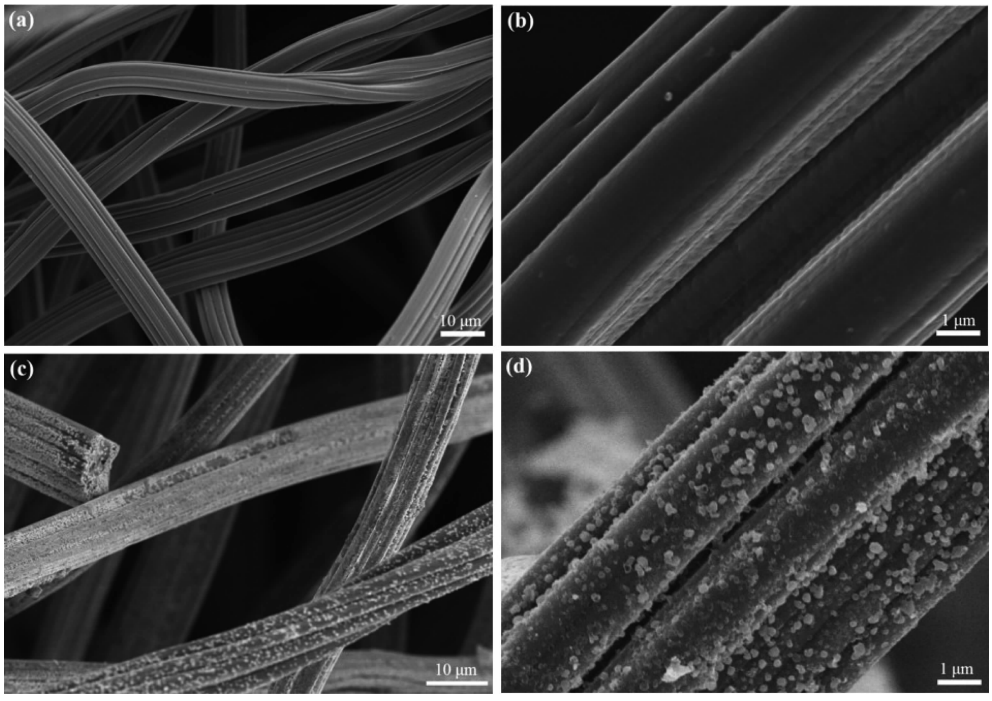

Fig.1 SEM images of GF (a, b) and CdO/GF (b, d) at different magnifications

GF, which proves that the CdO nanoparticle modification did not change the original structure of the graphite felt. CdO/GF also exhibited additional diffraction peaks at 32.6°, 37.9°, 54.4°, 65.6°, and 68.4°, which is consistent with the typical XRD pattern of CdO (JCPDS Card No.05-0640), and other peaks did not appear. These results confirmed that the CdO nanoparticles were successfully loaded onto the surface of the graphite felt fibers without changing their original structure.

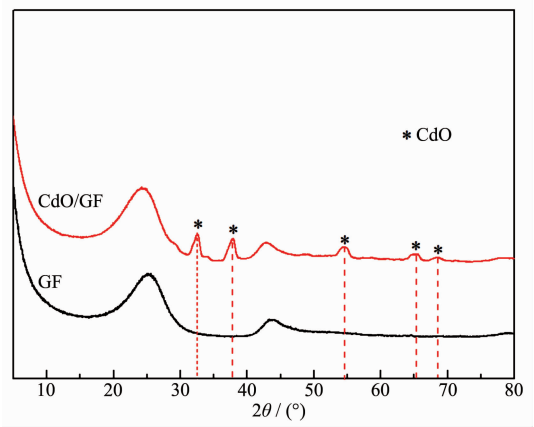

Fig.2 XRD pattern of GF and CdO/GF

2.2 Electrochemical characterization

Because the cadmium presented a high hydrogen evolution overpotential, the CdO/GF was expected to inhibit the activity of the HER. To experimentally verify this, the LSV test was performed to study the hydrogen evolution overpotential of electrodes. Fig.3 shows the LSV scan curves of GF and CdO/GF. It can be seen that the hydrogen evolution overpotential of GF is approximately −1.01 V, while the hydrogen evolution overpotential of CdO/GF is approximately −1.27 V, which increased by 0.26 V. The hydrogen evolution overpotential of CdO/GF is greatly improved relative to GF, which indicates that CdO has a certain inhibitory effect on the activity of the HER.

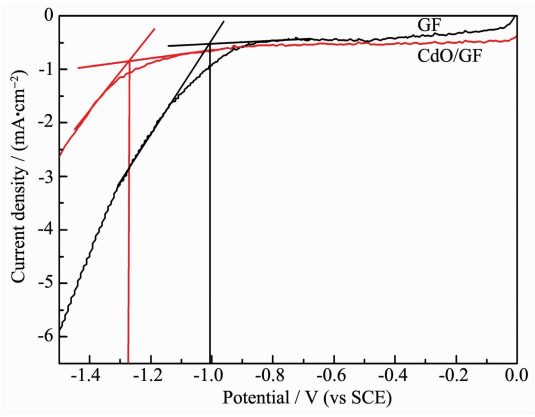

Fig.3 LSV curves of GF and CdO/GF in a solution of 0.05 mol·L^{-1} Na_2SO_4 at a scan rate of 5 mV·s^{-1}

Furthermore, a CV test was carried out to evaluate the electrocatalytic activity of the electrode towards the V^{3+}/V^{2+} redox couple. Fig.4 shows the CV curves for GF and CdO/GF. The anode peak corresponds to the oxidation process of V^{2+} to V^{3+}, and the cathode peak corresponds to the reduction process of V^{3+} to V^{2+}. In the case of the GF, the cathodic peak was not displayed, which can be ascribed to the high contribution of the HER. The CV curve of CdO/GF shows a distinct cathodic peak at approximately −0.75 V, and thus, it was verified that CdO/GF has a certain inhibitory effect on the activity of the HER. At the same time, the anodic current density of GF is approximately 18 mA·cm^{-2}, while CdO/GF is approximately 30 mA·cm^{-2}, which exhibits improvement of approximately 66.7%, indicating that CdO/GF has higher electrochemical activity than GF for the V^{3+}/V^{2+} redox reaction. Moreover, the potential of the anodic peak of the CV curve showed that GF appeared near −0.35 V, and CdO/GF appeared near −0.37 V, which implies that the reversibility of the V^{3+}/V^{2+} redox reaction is more optimal for the CdO/GF than that for GF. These results can be attributed to the well-deposited CdO nanoparticles, which play an important role as an electrocatalyst for the redox reaction of V^{3+}/V^{2+}.

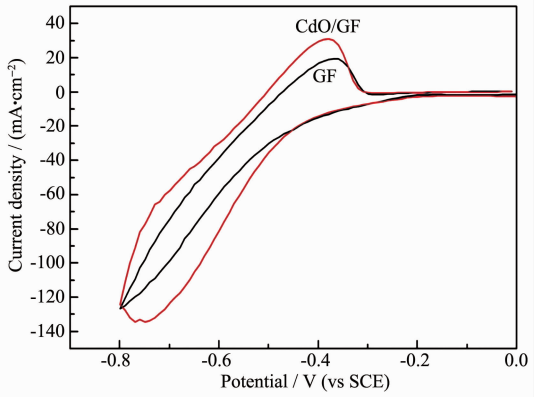

Fig.4 CV curves of GF and CdO/GF in a solution of 0.1 mol·L^{-1} $VOSO_4$ and 3 mol·L^{-1} H_2SO_4 at a scan rate of 5 mV·s^{-1}

The electrochemical properties of GF and CdO/GF was further investigated by EIS. Fig.5 shows the Nyquist plots of GF and CdO/GF. All the Nyquist plots consist of a semicircle at the high frequency and a linear component at low frequency. The semicircle in the high-frequency region corresponds to the charge transfer reaction at the electrolyte/electrode interface, and the inclined line at low frequency was attributed to Warburg impedance, which was induced in the ionic diffusion process in the pore channel of the electrode. The electrochemical process was mix-controlled by a charge transfer and diffusion steps. The intersection of the semicircle and the Z' axis represents the ohmic resistance (R_b) between the solution and the electrode, the radius of the semicircle in the high frequency region represents the charge transfer resistance (R_{ct})[35-36]. It can be seen that the R_b of CdO/GF is reduced compared to GF, indicating that the electrical conductivity of CdO/GF was more optimal than that of GF. In the presence of CdO, the R_{ct} of the CdO/GF significantly decreased with a R_{ct} of approximately 0.35 Ω, while the GF showed a R_{ct} of 0.60 Ω, indicating the positive effect of CdO/GF in the charge transfer rate of the V^{3+}/V^{2+} redox couple. Therefore, the electrochemical activity of CdO/GF was significantly enhanced by the introduction of CdO.

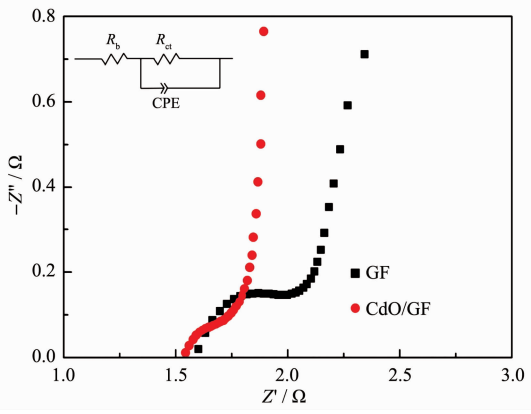

Fig.5　EIS of GF and CdO/GF in a solution of 0.1 mol·L^{-1} $VOSO_4$ and 3 mol·L^{-1} H_2SO_4 with an excitation signal of 10 mV under an open-circuit potential (OCP)

2.3　Single cell test

Due to the excellent electrochemical behavior of the CdO/GF electrode, the CdO/GF assembled in the VRFB single cell (cell A) and the cell performance were evaluated. To compare, the cell assembled with GF (cell B) was also measured. Both cells were evaluated using constant current charge-discharge tests.

The charge and discharge performance of cell A and cell B were measured at 60, 90, 120, and 150 mA·cm^{-2}. Fig.6a show the attenuation trend of the discharge capacity of cells A and B under different current densities. Cell B shows approximately 73.0% of the initial discharge capacity after 24 cycles. By contrast, cell A only possessed approximately 45.1% of the initial discharge capacity. It was observed that the higher the current density, the more obvious the enhancement effect. Fig.6b presents the energy efficiency (EE) of cells A and B tested at different currents. The EE of cell A at current density of 60 mA·cm^{-2} was approximately 76.8%, whereas for cell B, it was approximately 81.1%, which is approximately 4% higher than cell A. The EE of cell B remains higher than that of cell A at high current densities. The above experimental results are probably due to the inhibition of cadmium oxide on the activity of the HER, which reduces the energy loss of the battery. Fig.6c is a charge and discharge curve of cell A and cell B at a current density of 90 mA·cm^{-2}. The curve of cell B has a lower charge voltage plateau and a higher discharge voltage plateau compared with the curve of cell A. This indicates that cell B has lower electrochemical polarization resistance and higher voltage efficiency compared with cell A.

As long service life is vital for the practical VRFB, the stability of CdO/GF in the acidic electrolyte system of the VRFB was investigated. A test was conducted consisting of 100 charge-discharge cycles at a current density of 90 mA·cm^{-2} performed on cell B. As seen from Fig.6d~f, the coulombic efficiency (CE) of cell A was maintained at approximately 96.1%, whereas for cell B, it was maintained at approximately 97.1%. The increase of CE can be attributed to the CdO/GF, which suppressed the activity of HER. The voltage efficiency (VE) and EE of cell B were maintained at approximately 77.2% and 75.0%, respectively, whereas for cell A, they were only maintained

at approximately 72.3% and 69.5%, respectively. Also, the catalytic performance of CdO/GF maintained good stability during 100 cycles of a charge-discharge test.

The catalytic mechanism of CdO/GF for the V^{3+}/V^{2+} redox reaction is explained as shown in Fig.7. A large number of hydroxyl functional groups are located on the surface of the graphite felt fiber and CdO nanoparticles. During the charging process of the negative side solution of the VRFB, V^{3+} interacts with the hydroxyl groups, and the hydroxyl groups remove a proton into the solution and generate O-V bonds. After V^{3+} is reduced to V^{2+} by receiving an electron, O-V bonds are broken to obtain a proton from the solution that is reduced to the hydroxyl functional groups, and V^{2+} is returned to the solution. Similarly, during the discharge process, the reversed reaction occurs.

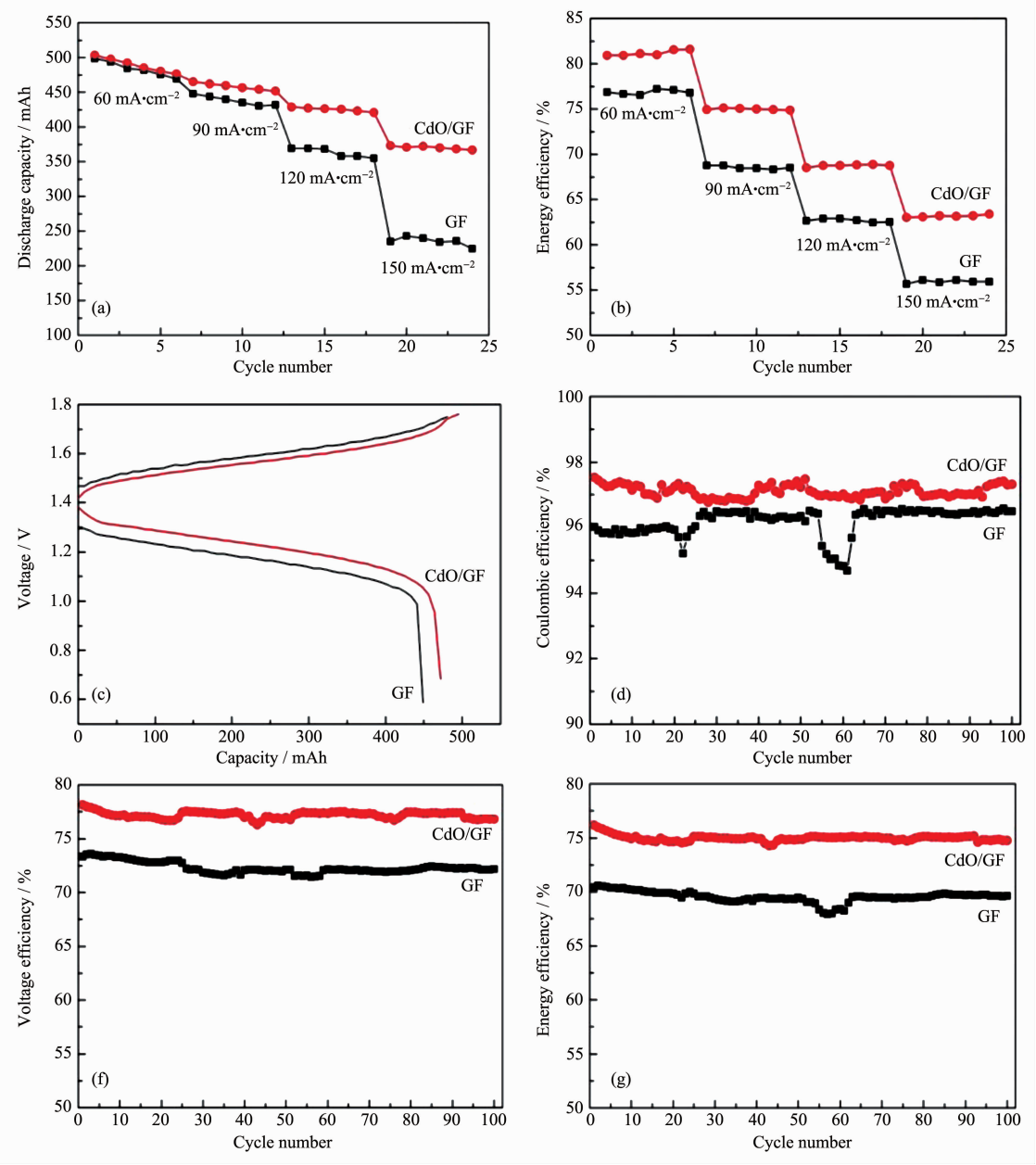

Fig.6 (a) Charging capacity attenuation trend and (b) energy efficiency of cell A and cell B at different current densities of 60, 90, 120, and 150 mA·cm^{-2}; (c) Charge-discharge curves of cell A and cell B at 90 mA·cm^{-2} current density; (d) Coulombic efficiency, (e) energy efficiency, and (f) voltage efficiency of 100 charge-discharge cycles for cell A and cell B at 90 mA·cm^{-2} current density

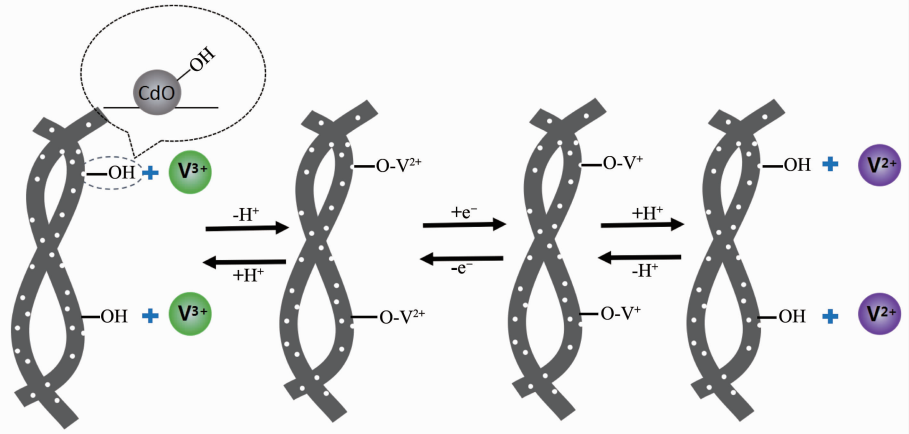

Fig.7　Catalytic reaction mechanism of CdO/GF as a negative electrode for VRFB

Because the electrolyte of VRFB is a strongly acidic solution, protons in the electrolyte are easily adsorbed on the surface of the GF fiber, and protons easily combine to form hydrogen gas. The HER is kinetically more favorable relative to the V^{3+}/V^{2+} redox reaction.

Using CdO/GF as negative electrode of the VRFB has the following advantages: (1) The CdO nanoparticles on the graphite felt fibers effectively inhibit the activity of the HER, and reduce the impact of the HER on VRFB performance. (2) Due to the presence of CdO nanoparticles, the number of hydroxyl functional groups on the surface of the graphite felt fibers increases, and the active site of the reaction increases, which results in an increase in the charge transfer rate between the electrode interface and V^{3+}. (3) Moreover, CdO is a wide bandgap n-type semiconductor. Due to the unique structure of the semiconductor band, the interface between the CdO/GF and the solution exhibits different properties from the general electrode. The products formed by the reaction do not easily accumulate on the surface of the electrode, which greatly increases the reaction rate.

3　Conclusions

In order to improve the electrocatalytic activity of GF towards the V^{3+}/V^{2+} redox couple and inhibit the activity of the HER, CdO/GF were synthesized for the first time using a hydrothermal method. Compared with the original graphite felt, the CdO/GF effectively inhibited the activity of the HER, showed increased electrochemical activity and reversibility for the V^{3+}/V^{2+} redox couple, and the charge transfer resistance was also significantly reduced. When CdO/GF was used as the negative electrode of a VRFB, the decay rate of the charge capacity significantly reduced, the energy efficiency (EE) was also significantly improved. The catalytic performance of CdO/GF can confer good stability during 100 constant current charge-discharge tests, and the VE and EE of CdO/GF were approximately 5% higher than GF at a current density of 90 mA·cm^{-2}. Futhermore, a catalytic reaction mechanism that explains the role of CdO nanoparticles for the V^{3+}/V^{2+} redox reaction has been proposed. In conclusion, CdO/GF has good application prospects as negative electrode for VRFB.

References:

[1] Parasuramana A, Lim T M, Menictas C, et al. *Electrochim. Acta*, **2013**,**101**:27-40

[2] Kim K J, Park M S, Kim Y J, et al. *J. Mater. Chem. A*, **2015**, **3**:16913-16933

[3] Bayeh A W, Kabtamu D M, Chang Y C, et al. *ACS Sustainable Chem. Eng.*, **2018**,**6**:3019-3028

[4] Larcher D, Tarascon J M. *Nat. Chem.*, **2015**,**7**:19-29

[5] Fu S F, Zhu C Z, Song J H, et al. *Electroanal.*, **2017**,**29**: 1469-1473

[6] Zhang Z Y, Xi J Y, Zhou H P, et al. *Electrochim. Acta*, **2016**,**218**:15-23

[7] Skyllas-Kazacos M, Chakrabarti M H, Hajimolana S A, et al. *J. Electrochem. Soc.*, **2011**,**158**:R55-R79

[8] Xiao S B, Yu L H, Wu L T, et al. *Electrochim. Acta*, **2016**,

187:525-534

[9] Yuan Z Z, Zhu X X, Li M R, et al. *Angew. Chem. Int. Ed.*, **2016**,**55**:3058-3062

[10]Kabtamu D M, Chen J Y, Chang Y C, et al. *J. Power Sources*, **2017**,**341**:270-279

[11]He Z X, Jiang Y Q, Meng W, et al. *Appl. Surf. Sci.*, **2017**, **423**:111-118

[12]Wei L, Zhao T S, Zhao G, et al. *Appl. Energy*, **2016**,**176**:74-79

[13]Chakrabarti M H, Brandon N P, Hajimolana S A, et al. *J. Power Sources*, **2014**,**253**:150-166

[14]Jiang H R, Shyy W, Wu M C, et al. *J. Power Sources*, **2017**, **365**:34-42

[15]He Z X, Jiang Y Q, Meng W, et al. *Appl. Surf. Sci.*, **2017**, **423**:111-118

[16]Flox C, Rubio-García J, Skoumal M, et al. *Carbon*, **2013**,**60**: 280-288

[17]Zhang W G, Xi J Y, Li Z H, et al. *Electrochim. Acta*, **2013**, **89**:429-435

[18]Wondimu T H, Chen G C, Kabtamu D M, et al. *Int. J. Hydrogen. Energy*, **2018**,**43**:6481-6490

[19]He Z X, Jiang Y Q, Wei Y L, et al. *Electrochim. Acta*, **2018**,**259**:122-130

[20]Wu X X, Xu H F, L L, et al. *J. Power Sources*, **2014**,**250**: 274-278

[21]Shen Y, Xu H F, Xu P C, et al. *Electrochim. Acta*, **2014**, **132**:37-41

[22]Shi L, Liu S Q, He Z, et al. *Electrochim. Acta*, **2015**,**178**: 748-757

[23]He Z X, Dan Lei, Liu S Q, et al. *Electrochim. Acta*, **2015**, **176**:1434-1440

[24]Li W Y, Zhang Z Y, Tang Y B, et al. *Adv. Sci.*, **2016**,**3**: 1500276

[25]Suárez D J, González Z, Blanco C, et al. *ChemSusChem*, **2014**,**7**:914-918

[26]Vázquez-Galván J, Flox C, Fàbrega C, et al. *ChemSusChem*, **2017**,**10**:2089-2098

[27]Ventosa E, Skoumal M, Vazquez F J, et al. *J. Power Sources*, **2014**,**271**:556-560

[28]Kabir H, Gyan I O, Cheng I F. *J. Power Sources*, **2017**,**342**: 31-37

[29]Shah A A, Al-Fetlawi H, Walsh F C. *Electrochim. Acta*, **2010**,**55**:1125-1139

[30]Chen F Y, Liu J G, Chen H, et al. *Int. J. Electrochem. Sci.*, **2012**,**7**:3750-3764

[31]Li B, Gu M, Nie Z, et al. *Nano Letters*, **2013**,**13**(3):1330-1335

[32]Liu Y C, Liang F, Zhao Y, et al. *J. Energy Chem.*, **2018**,**27**: 1333-1340

[33]Creighton H J. *Principle and applications of Electrochemistry*. New York: John Wiley & Sons, **1948**:248

[34]XU Qian(许茜), QIAO Yong-Lian(乔永莲). *Chinese J. Power Sourses*(电源技术), **2008**,**32**(12):823-826

[35]Li B, Gu M, Nie Z M, et al. *Nano Lett.*, **2014**,**14**:158-165

[36]Zhou H P, Xi J Y, Li Z H, et al. *RSC Adv.*, **2014**,**4**:61912-61918